CHIN. PHYS. LETT. Vol. 38, No. 3 (2021) 036201

Novel Superconducting Electrides in Ca–S System under High Pressures

Yun-Xian Liu(刘云仙), Chao Wang(王超)*, Shuai Han(韩帅), Xin Chen(陈欣), Hai-Rui Sun(孙海瑞), and Xiao-Bing Liu(刘晓兵)*

Laboratory of High Pressure Physics and Material Science (HPPMS), School of Physics and Physical Engineering, Qufu Normal University, Qufu 273165, China

(Received 22 December 2020; accepted 19 January 2021; published online 2 March 2021)

Due to their unique structure properties, most of the electrides that possess extra electrons locating in interstitial regions as anions are insulators. Metallic and superconducting electrides are very rare under ambient conditions. We systematically search possible compounds in Ca–S systems stabilized under various pressures up to 200 GPa, and investigate their crystal structures and properties using first-principles calculations. We predict a series of novel stoichiometries in Ca–S systems as potential superconductors, including $P2_1/m$ Ca_3S, $P4mbm$ Ca_3S, Pnma Ca_2S, $Cmcm$ Ca_2S, $Fddd$ CaS_2, $Immm$ CaS_3 and $C2/c$ CaS_4. The $P4mbm$ Ca_3S phase exhibits a maximum T_c value of ∼20 K. It is interesting to notice that the $P2_1/m$ Ca_3S and $Pnma$ Ca_2S stabilized at 60 and 50 GPa behave as superconducting electrides with critical temperatures T_c of 7.04 K and 0.26 K, respectively. More importantly, our results demonstrate that $P2_1/m$ Ca_3S and $Pnma$ Ca_2S are dynamically stable at 5 GPa and 0 GPa, respectively, indicating a high possibility to be quenched to ambient condition or synthesized using the large volume press.

DOI: 10.1088/0256-307X/38/3/036201

Superconducting materials exhibit peculiar physical properties, which can be applied in energy, defense, transportation, computer technology and medicine. Since the discovery of superconductors, exploring new high temperature superconductors has been a hot topic in the fields of condensed matter physics and materials science. To date, cuprates,[1] iron pnictides,[2–4] hydrides[5–6] and some 2D compounds[7–11] have been reported. Although considerable research and understanding of superconductors have been greatly progressed, it is a long way to seek new high temperature superconductors which can be experimentally synthesized and available at room temperature.

Electrides are extraordinary compounds with extra electrons locating in interstitial regions as anions.[12–13] Under ambient conditions, metallic and superconducting electrides are very rare. Among a few superconducting candidates, previous electrides are reported to exhibit low superconducting transition temperature T_c, such as $[Ca_{24}Al_{28}O_{64}]^{4+}(e^-)_4$ (C12A7:e^-)$^-$,[14] Mn_5Si_3-type Nb_5Ir_3,[15] Y_2C and MgONa.[16] Further exploration of new superconducting electrides can be helpful for deep understanding their formation mechanisms and superconducting behavior.

Since energies of both the interstitial and atomic orbitals are sensitive to pressure conditions, high-pressure techniques have been found to be a powerful way to synthesize novel electrides by effectively shortening the atomic spacing and increasing the overlap of adjacent electron orbitals to overcome high formation energy barriers.[13,17–18] Previous experimental and theoretical studies have reported that a series of electrides of elements (Li, Na, K and Mg) and related compounds [$NaHe_2$, Mg_3O_2, Mg–NG (NG = Xe, Kr, Ar), Li_nI, Al_2S and Ca_3Si] have already been stabilized under high pressures, exhibiting exotic properties as metallic-semiconductor-insulator transition, superconductivity.[13,19–28] Recently, it is striking that a pressure-induced electride as Li_6P compound exhibits a highest T_c value of 39.3 K among all already known electrides.[29] Such a value is even higher than that of some conventional superconducting systems,[1–4] indicating a new way to search for high temperature superconductors. Nevertheless, the expense of trial-and-error synthesis under extremely high pressure condition (270 GPa) for the phase stabilization has severely hampered the deep investigation of detailed mechanism, much less to its potential commercial applications in the future. It is therefore of great importance to investigate novel superconducting electride systems under relatively low pressure conditions. On the other hand, most of the pressure-stabilized electrides are metastable materials and can be conserved after releasing the pressure, thus exploration for stable phases at ambient pressure is also highly deserved for practical applications.

Supported by the National Natural Science Foundation of China (Grant Nos. 11704220, 11804184, 11974208 and 11804185), the Shandong Provincial Natural Science Foundation (Grant Nos. ZR2017BA020, ZR2018PA010, ZR2019MA054 and ZR2017BA012).
*Corresponding authors. Email: wangchao0531608@163.com; xiaobing.phy@qfnu.edu.cn
© 2021 Chinese Physical Society and IOP Publishing Ltd

Previous studies have found that compounds consisting of elements with small electronegativity and large atomic radii are more likely to form electrides, including alkali metals, alkaline-earth metals and early transition metals in group ⅢB.[30,31] In particular, the alkaline earth metal element, Ca, occurs more frequently than others. Additionally, considering that S can be comparable to P in electronegativity, we expect that Ca–S systems would have high possibility to realize electrides with superconductivity. Here, we systematically search the possible compounds in Ca–S systems under various pressure, and investigate their crystal structures and properties using first-principles calculations. A series of novel stoichiometries are found in Ca–S systems as potential superconductors, including $P2_1/m$ Ca_3S, $P4mbm$ Ca_3S, $Pnma$ Ca_2S, $Cmcm$ Ca_2S, $Fddd$ CaS_2, $Immm$ CaS_3 and $C2/c$ CaS_4. The $P4mbm$ Ca_3S phase exhibits a maximum T_c value of ∼20 K. Moreover, it is interesting to notice that the $P2_1/m$ Ca_3S and $Pnma$ Ca_2S behave as superconducting electrides, which can be quenched to ambient conditions.

Computational Details. We have explored the pressure-induced structural evolution in Ca–S systems with various Ca_mS_n ($m = n =$ 1–4) using the CALYPSO (Crystal structure AnaLYsis by Particle Swarm Optimization)[32–33] and USPEX (Universal Structure Predictor: Evolutionary Xtallography) codes[34–44] at temperature of 0 K and at pressures of 0, 50, 100, 150 and 200 GPa. Such methods have been successfully employed in various systems.[37–55] We performed structural optimization and electronic structure calculations using the Vienna *ab initio* simulation package (VASP)[56] based on density functional theory (DFT), within the Perdew–Burke–Ernzerhof (PBE) version of generalized gradient approximation (GGA).[57] The projector-augmented-wave potentials (PAWs)[58] have been adopted, with $3p^64s^2$ and $3s^23p^4$ treated as valence electrons for Ca and S atoms, respectively. To ensure that total energy calculations were converged to less than 1 meV, we used the cutoff energy of 500 eV and fine Monkhorst–Pack k-meshes of $2\pi \times 0.025$ Å^{-1}. We determined dynamic stability by calculating the phonon using a supercell approach with the finite displacement approach,[59] as implemented in the PHONOPY code.[60] We used the electron localization function (ELF)[61] and Bader's Quantum Theory of Atoms in Molecules (QTAIM) analysis[62–64] to analyze the degree of electron localization, and electronic charge transfer calculations are tested by the VASP code. The crystal orbital Hamilton populations (COHP)[65,66] was calculated using the LOBSTER code,[67] to analyze the interatomic interaction and chemical bonding. The electron–phonon coupling (EPC) calculations were performed using the Quantum ESPRESSO (QE) package.[68] The norm-conserving pseudopotentials and a kinetic energy cutoff of 90 Ry were employed.

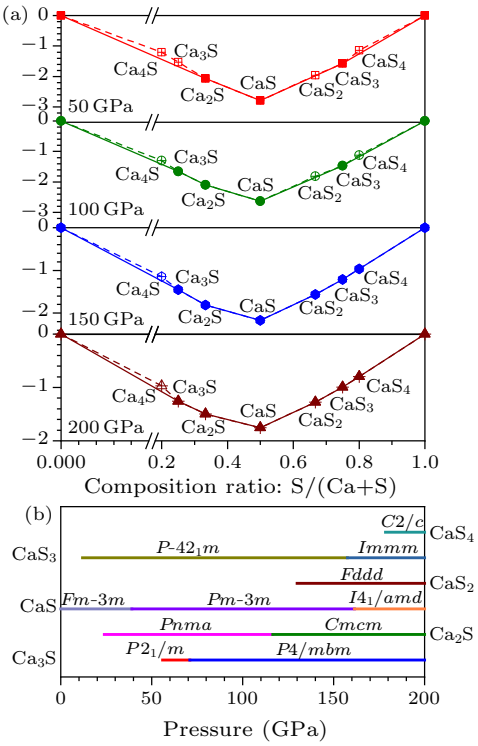

Fig. 1. Thermodynamic stabilities and stable pressure ranges of Ca_mS_n compounds. (a) Formation enthalpies (ΔH) per atom of the Ca_mS_n phases with respect to their separated counterparts at 0 K and at different pressures. (b) Pressure ranges in which the corresponding phases of different Ca–S compounds are thermodynamically stable.

Results and Discussion. To investigate the phase stability of Ca–S systems, the thermodynamic stabilities were evaluated by calculating their formation enthalpies (ΔH) with respect to constituent elements. As references, the energetically most favorable structures of face-centered-cubic, body-centered-cubic, and β-tin phases for Ca, $I4_1/acd$ and β-Po phases for S were adopted in their corresponding stable pressure ranges. To account for the enthalpy relationships and all possible formation routes of each stoichiometry, we constructed the convex hulls for the Ca–S binary compounds at 0 and 50, 100, 150, and 200 GPa, as shown in Fig. 1(a) and Fig. S1 in the Supplementary Information. Formation enthalpies of compounds are located on the hull (solid lines), showing thermodynamically stability with relative to other binary stoichiometries or elements, while other phases located above the hull (dashes lines) are either unstable or metastable. At ambient conditions, CaS is the only stable stoichiometry, in agreement with the experimental results, and it remains stable to 200 GPa. With increasing pressure to 50 GPa, Ca_2S and CaS_3 are found to be stable. Upon further compression, Ca_3S gradually becomes stable with respect to decomposition into other compounds at 100 GPa. At 150 and 200 GPa, exception of

the Ca_4S stoichiometry, all the other compounds are energetically favored over element. The present finding demonstrates that high pressure clearly favors the formation of Ca–S compounds.

The predicted pressure ranges of thermodynamic stability for Ca–S are presented in Fig. 1(b). For CaS, the well-known structure $Fm\bar{3}m$ under ambient conditions was predicted to be stable till 39 GPa. Then it transforms into $Pm\bar{3}m$ and $I4_1/amd$ at 39 and 161.5 GPa, respectively. We find that Ca_3S is stable in monoclinic $P2_1/m$ structure in pressure ranges of 56–71 GPa, then a tetragonal $P4/mbm$ phase is energetically favorable. Turning to Ca_2S, *Pnma* is the most stable phase between 24 and 116.7 GPa, and then it is overtaken by an energetically favored *Cmcm* structure up to 200 GPa. For CaS_2 stoichiometry, the *Fddd* structure becomes favorable from 130 to 200 GPa. For CaS_3, $P\bar{4}2_1m$ is stable in a pressure range from 12 to 158 GPa, then *Immm* becomes more favored. For the CaS_4 compound, the predicted $C2/c$ is energetically stable above 178.5 GPa. Since the dynamical stability is one of the basic requirements for structures, we have calculated their phonon spectra for Ca–S compounds, as shown in Figs. S2 and S3 in the Supplementary Information. It is clear that the calculated phonon dispersion curves show no imaginary phonon frequency in the entire Brillouin zone for all the predicted structures, indicating that they are dynamically stable in the corresponding stable pressure ranges.

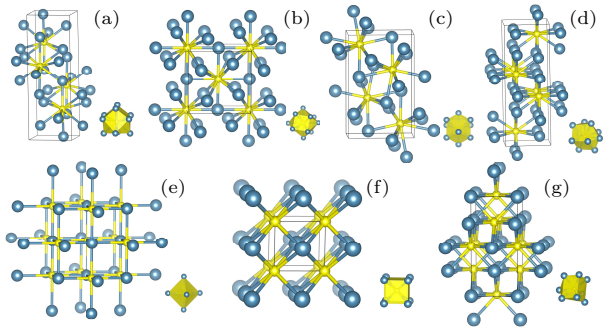

Fig. 2. Predicted stable crystal structures of studied Ca-rich compounds under pressure: (a) $P2_1/m$ Ca_3S at 50 GPa, (b) $P4/mbm$ Ca_3S at 200 GPa, (c) *Pnma* Ca_2S at 100 GPa, (d) *Cmcm* Ca_2S at 200 GPa, (e) $Fm\bar{3}m$ CaS at 0 GPa, (f) $Pm\bar{3}m$ CaS at 100 GPa, (g) $I4_1/amd$ CaS at 200 GPa. Bice and yellow balls denote Ca and S atoms, respectively.

Figure 2 illustrates the crystal structures for the predicted stable Ca-rich compounds. For Ca_3S, it is observed that the $P2_1/m$ structure consists of Ca-sharing SCa_{10} polygons [Fig. 2(a)], while in the $P4/mbm$ Ca_3S phase, each S atom is surrounded by 12 Ca [Fig. 2(b)]. It is a common phenomenon that the coordination number increases under high pressure. Ca_2S exhibits two orthorhombic structures *Pnma* [Fig. 2(c)] and *Cmcm* [Fig. 2(d)], in which each S is surrounded by ten Ca atoms and the nearest Ca–S distance varies from 2.42 to 2.31 Å with the increased pressure. For CaS, the well-known semiconducting $Fm\bar{3}m$ structure and new cubic $Pm\bar{3}m$ phases were predicted, which could be viewed as NaCl-type and CsCl-type [Figs. 2(e) and 2(f)], respectively. The high-pressure stable $I4_1/amd$ CaS phase is found to be composed of Ca-sharing SCa_8 polygons with a closest Ca–S distance of 2.34 Å, as depicted in Fig. 2(g). It should be pointed out that, compared to the well-known semiconducting $Fm\bar{3}m$ CaS structure, the Ca-rich phases possess higher coordination number and denser polyhedral packing, which may result in distinct electronic properties.

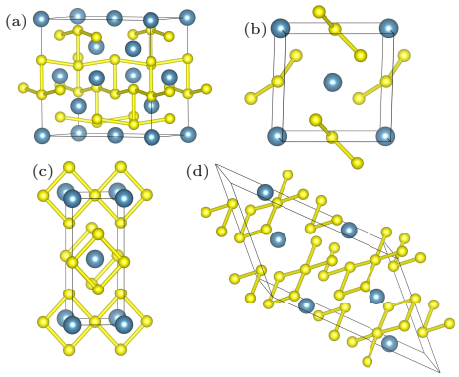

Fig. 3. Predicted stable crystal structures of studied S-rich compounds under pressure: (a) *Fddd* CaS_2 at 200 GPa, (b) $P\bar{4}2_1m$ CaS_3 at 100 GPa, (c) *Immm* CaS_3 at 200 GPa, (d) $C2/c$ CaS_4 at 200 GPa.

Then it turns to the predicted S-Rich compounds. In the *Fddd* CaS_2 structure, we observe folded layers formed by sulfur atoms, between which S–S bonds exist. They form the three-dimensional network [Fig. 3(a)]. There are two distances between closest S–S of 2.18 and 2.05 Å. With the increase of S, the CaS_3 with $P\bar{4}2_1m$ symmetry is constituted by S_3 units and isolated Ca atoms [Fig. 3(b)]. Moreover, it is interesting to notice that the *Immm* CaS_3 phase is formed by alternating four-grid chains (composed of S) and Ca atoms [Fig. 3(c)]. For the S-richest compound, sulfur atoms in the predicted $C2/c$ CaS_4 structure form fence with the S–S distances of 2.08 and 2.04 Å [Fig. 3(d)]. From the calculated electron localization function (ELF), it can be seen in Figs. S4 and S5 that high ELF values for S-rich compounds are distributed between S atoms, indicating the presence of S–S covalent bonds. Moreover, we calculated their integrated-crystal orbital Hamilton populations (ICOHPs) to scale the bond strength in compounds by counting the energy-weighted population of wave function between two atomic orbitals. Our results demonstrate that the forming S–S interaction strength is much larger than that of Ca–S bonds. For example, the value of ICOHP of S–S and Ca–S are 3.19 and 0.45 eV per pair in the $C2/c$ CaS_4, respectively. Therefore, we conclude that the S–S interactions are

mainly responsible for the structural stabilities in the S-rich compositions.

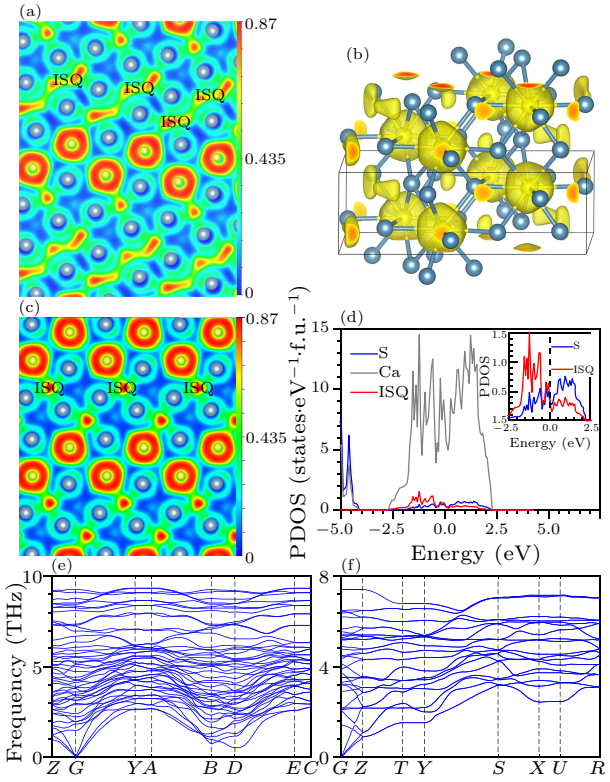

Fig. 4. Electronic and dynamic properties of $P2_1/m$ Ca_3S and *Pnma* Ca_2S: (a) the calculated 2D ELF in (010) plane, (b) 3D ELF plot with an isosurface value of 0.65 for $P2_1/m$ Ca_3S at 60 GPa, (c) 2D ELF for *Pnma* Ca_2S at 50 GPa, (d) the projected density of states (PDOS) for $P2_1/m$ Ca_3S at 60 GPa, (e) the calculated phonon dispersion curves of $P2_1/m$ Ca_3S at 5 GPa, (f) *Pnma* Ca_2S at 0 GPa.

Among all our predicted stable phases, it is interesting to notice that the *Pnma* Ca_2S and $P2_1/m$ Ca_3S compounds behave as electrides. Therefore, we mainly focus on the analysis and discussion about the two phases of the *Pnma* Ca_2S and $P2_1/m$ Ca_3S in the following. Figures 4(a) and 4(c) show the calculated two-dimensional (2D) ELF in (010) plane for *Pnma* Ca_2S at 50 GPa and for $P2_1/m$ Ca_3S at 60 GPa, respectively. To clearly observe the distribution of electron, the three-dimensional (3D) ELF plot with an isosurface value of 0.65 for $P2_1/m$ Ca_3S is also shown in Fig. 4(b). It can be clearly seen that extra electrons locate at the positions of interstitial regions, which can be regarded as interstitial quasi-atoms (ISQs). In addition, we calculated the Bader charges for $P2_1/m$ Ca_3S, and found that nearly two electrons reside in the interstitials. Such behavior provides strong evidence for *Pnma* Ca_2S and $P2_1/m$ Ca_3S as electrides.[12,13] More importantly, our results demonstrate that both the *Pnma* Ca_2S and $P2_1/m$ Ca_3S electrides exhibit metallic behavior. It is well known that the interstitial electrons can occupy shallow bands and largely determine the physical properties. Figure 4(d) gives the calculated projected density of states (PDOS) of the $P2_1/m$ Ca_3S. We found that, although the main contribution near the Fermi level (E_F) is from Ca, the contribution of interstitial electrons to the metallic state is also important. Moreover, it is striking to note that the electrides of $P2_1/m$ Ca_3S and *Pnma* Ca_2S were also predicted to be dynamically stable at 5 GPa and 0 GPa [Figs. 4(e) and 4(f)] from the calculated phonon spectra. Such results provide high possibility for the high pressure phases to be quenched to ambient condition or synthesized using the large volume press at industrial scale production for practical applications.

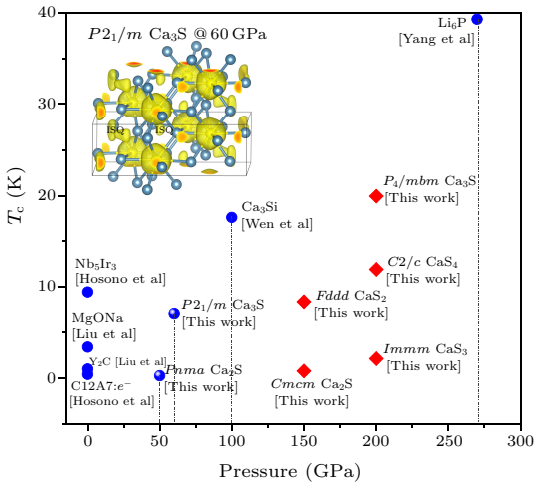

Fig. 5. The calculated values of T_c for different electrides in the pressure range from 0 to 300 GPa. Insert: 3D ELF plot for $P2_1/m$ Ca_3S at 60 GPa. Blue balls and red rhombus denote electrides and superconductors, respectively.

Motivated by their metallic behavior and high stability, we further explored their possible superconductivity of $P2_1/m$ Ca_3S and *Pnma* Ca_2S. Their superconducting critical temperatures (T_c) are evaluated through electron–phonon coupling (EPC) calculations, which is based on the Allen–Dynes-modified McMillan equation:[69]

$$T_c = \frac{\omega_{\log}}{1.2} \exp\left[\frac{1.04(1+\lambda)}{\lambda - \mu^*(1+0.62\lambda)}\right].$$

Other stable phases with metallic properties in the Ca–S systems are also included for comparison (Table 1). With the Coulomb parameter set $\mu^* = 0.1$, seven stoichiometries were predicted as potential superconductors, including $P2_1/m$ Ca_3S, $P4mbm$ Ca_3S, *Pnma* Ca_2S, *Cmcm* Ca_2S, *Fddd* CaS_2, *Immm* CaS_3 and $C2/c$ CaS_4. The $P4mbm$ Ca_3S phase exhibits a maximum T_c value of ∼20 K. More importantly, we note that the two stable electrides of $P2_1/m$ Ca_3S and *Pnma* Ca_2S phases exhibit T_c values of 7.04 and 0.26 K, respectively. The details are summarized in Fig. 5. Notably, it is clear that the relatively low pressure conditions (50–60 GPa)

are needed for the stabilization of the $P2_1/m$ Ca_3S and $Pnma$ Ca_2S phases among the known pressure-induced electrides in previous theoretical and experimental results.[12,19,21,28,29] Further calculations found that the compounds of Ca_3S and Ca_2S can be formed not only by elements Ca and S, but also by CaS and Ca ($Ca + CaS \rightarrow Ca_2S/Ca_3S$). Taking into account of their quenchable behavior, we suggest that such new superconducting electrides are highly valuable for further research and possess a high possibility to be synthesized.

Table 1. The calculated value of λ, the logarithmic average phonon frequency $\omega_{\log}$, electronic density of states at the Fermi level $N(E_F)$ (states·spin^{-1}·Ry^{-1}·f.u.$^{-1}$), and superconducting critical temperatures T_c for Ca–S compounds.

Structures	Pressure (GPa)	λ	$\omega_{\log}$ (K)	N(E_F)	T_c (K) for $\mu^* = 0.1$	Type
$P2_1/m$ Ca_3S	60	0.71	193.24	47.54	7.04	Electride
$P4/mbm$ Ca_3S	200	1.11	246.53	16.03	19.93	Superconductor
$Pnma$ Ca_2S	50	0.32	289.03	36.82	0.26	Electride
$Cmcm$ Ca_2S	150	0.35	412.24	13.16	0.78	Superconductor
$I4_1/amd$ CaS	200	0.25	283.67	2.19	0.016	Superconductor
$Fddd$ CaS_2	150	1.03	114.37	11.87	8.33	Superconductor
$Immm$ CaS_3	200	0.40	532.46	6.03	2.13	Superconductor
$C2/c$ CaS_4	200	0.63	460.16	18.11	11.88	Superconductor

In summary, the variable stoichiometries and properties of Ca–S system have been systematically explored under pressure up to 200 GPa. Six pressure-induced Ca–S compounds are found. The results show that $P2_1/m$ Ca_3S, $P4mbm$ Ca_3S, $Pnma$ Ca_2S, $Cmcm$ Ca_2S, $Fddd$ CaS_2, $Immm$ CaS_3 and $C2/c$ CaS_4 are superconductors with the T_c of 7.04, 19.93, 0.26, 0.78, 8.33, 2.13, 11.88 K at different pressures, respectively. Furthermore, we find that the pressure-induced superconducting compounds of $P2_1/m$ Ca_3S and $Pnma$ Ca_2S become electrides at 60 and 50 GPa. These two electrides are dynamically stable at 5 and 0 GPa, showing quenchable under ambient conditions. Our findings provide a feasible direction for future experimental study on Ca–S systems under pressure.

Some of the calculations were performed in the High Performance Computing Center (HPCC) of Qufu Normal University.

References

[1] Cava R J, Van Dover R B, Batlogg B and Rietman E A 1987 *Phys. Rev. Lett.* **58** 408
[2] Kamihara Y, Watanabe T, Hirano M *et al.* 2008 *J. Am. Chem. Soc.* **130** 3296
[3] Hsu F C, Luo J Y, Yeh K W *et al.* 2008 *Proc. Natl. Acad. Sci. USA* **105** 14262
[4] Mizuguchi Y, Tomioka F, Tsuda S *et al.* 2008 *Appl. Phys. Lett.* **93** 152505
[5] Sun Y, Lv J, Xie Y, Liu H and Ma Y M 2019 *Phys. Rev. Lett.* **123** 097001
[6] Xie H, Yao Y, Feng X *et al.* 2020 *Phys. Rev. Lett.* **125** 217001
[7] Shi W, Yu J, Xu T *et al.* 2021 *Sci. Chin. Mater.* **64** 664
[8] Chen J 2021 *J. Supercond. Nov. Magn.* (in press)
[9] Yang C, Liu Y and Wang Y 2019 *Science* **366** 1505
[10] Wang X, Li H and Dong Z 2019 *Acta Phys. Sin.* **68** 027401 (in Chinese)
[11] Liang C, Zhang J and Zhao K 2020 *Acta Phys. Sin.* **69** 237401 (in Chinese)
[12] Miao M S and Hoffmann R 2014 *Acc. Chem. Res.* **47** 1311
[13] Miao M S, Wang X L and Brgoch J 2015 *J. Am. Chem. Soc.* **137** 14122
[14] Miyakawa M, Kim S W and Hirano M 2007 *J. Am. Chem. Soc.* **129** 7270
[15] Zhang Y, Wang B and Xiao Z 2017 *npj Quantum Mater.* **2** 45
[16] Ge Y, Guan S and Liu Y 2017 *New J. Phys.* **19** 123020
[17] Wang J, Hanzawa K and Hiramatsu H 2017 *J. Am. Chem. Soc.* **139** 15668
[18] Lu Y, Li J and Tada T 2016 *J. Am. Chem. Soc.* **138** 3970
[19] Matsuoka T and Shimizu K 2009 *Nature* **458** 186
[20] Pickard C J and Needs R J 2009 *Phys. Rev. Lett.* **102** 146401
[21] Ma Y, Eremets M, Oganov A R *et al.* 2009 *Nature* **458** 182
[22] Pickard C J and Needs R J 2011 *Phys. Rev. Lett.* **107** 087201
[23] Li P, Gao G and Wang Y 2010 *J. Phys. Chem. C* **114** 21745
[24] Dong X, Oganov A R, Goncharov A F *et al.* 2017 *Nat. Chem.* **9** 440
[25] Zhu Q, Oganov A R and Lyakhov A O 2013 *Phys. Chem. Chem. Phys.* **15** 7696
[26] Botana J, Brgoch J, Hou C *et al.* 2016 *Inorg. Chem.* **55** 9377
[27] Shao S, Zhu W, Lv J *et al.* 2020 *npj Comput. Mater.* **6** 11
[28] Sa B, Xiong R, Wen C *et al.* 2020 *J. Phys. Chem. C* **124** 7683
[29] Zhao Z, Zhang S and Yu T 2019 *Phys. Rev. Lett.* **122** 097002
[30] Zhang Y, Wang H, Wang Y, Zhang L and Ma Y 2017 *Phys. Rev. X* **7** 011017
[31] Zhu Q, Frolov T and Choudhary K 2019 *Matter* **1** 1293
[32] Wang Y, Lv J and Zhu L 2010 *Phys. Rev. B* **82** 094116
[33] Wang Y, Lv J and Zhu L 2012 *Comput. Phys. Commun.* **183** 2063
[34] Oganov A R and Glass C W 2006 *J. Chem. Phys.* **124** 244704
[35] Oganov A R, Lyakhov A O and Valle M 2011 *Acc. Chem. Res.* **44** 227
[36] Lyakhov A O, Oganov A R and Stokes H T 2013 *Comput. Phys. Commun.* **184** 1172
[37] Chu B H, Zhao Y, Yan J L *et al.* 2018 *Chin. Phys. Lett.* **35** 016401
[38] Sun G L, Huang H M and Li Y L 2016 *Chin. Phys. Lett.* **33** 026104
[39] Wang C, Liu Y X, Chen X *et al.* 2020 *Chin. Phys. Lett.* **37** 026201
[40] Qu N R, Wang H C, Li Q *et al.* 2019 *Chin. Phys. Lett.* **36** 036201
[41] Cang Y P, Lian S B, Yang H M *et al.* 2016 *Chin. Phys. Lett.* **33** 066301
[42] Wu J H and Liu C X 2016 *Chin. Phys. Lett.* **33** 036202

[43] Zhou D, Zheng Y, Pu C *et al.* 2018 *Chin. Phys. Lett.* **35** 107101
[44] Zhang S, He J, Zhao Z *et al.* 2019 *Chin. Phys. B* **28** 106104
[45] Liu G, Yu Z, Liu H *et al.* 2018 *J. Phys. Chem. Lett.* **9** 5785
[46] Peng F, Botana J, Wang Y *et al.* 2016 *J. Phys. Chem. Lett.* **7** 4562
[47] Kruglov I A, Semenok D V, Song H *et al.* 2020 *Phys. Rev. B* **101** 024508
[48] Rybkovskiy D V, Kvashnin A G, Kvashnina Y A *et al.* 2020 *J. Phys. Chem. Lett.* **11** 2393
[49] Wan B, Zhang J, Wu L *et al.* 2019 *Chin. Phys. B* **28** 106201
[50] Tong Q, Lv J, Gao P *et al.* 2019 *Chin. Phys. B* **28** 106105
[51] Tian Y, Sun W, Chen B *et al.* 2019 *Chin. Phys. B* **28** 103104
[52] Tang C, Kour G and Du A 2019 *Chin. Phys. B* **28** 107306
[53] Lin J, Du X and Yang G 2019 *Chin. Phys. B* **28** 106106
[54] Hermann A 2019 *Chin. Phys. B* **28** 106107
[55] Cui W and Li Y 2019 *Chin. Phys. B* **28** 107104
[56] Kresse G and Furthmüller J 1996 *Comput. Mater. Sci.* **6** 15
[57] Perdew J P, Burke K and Ernzerhof M 1996 *Phys. Rev. Lett.* **77** 3865
[58] Kresse G and Joubert D 1999 *Phys. Rev. B* **59** 1758
[59] Parlinski K, Li Z and Kawazoe Y 1997 *Phys. Rev. Lett.* **78** 4063
[60] Togo A, Oba F and Tanaka I 2008 *Phys. Rev. B* **78** 134106
[61] Becke A D and Edgecombe K E 1990 *J. Chem. Phys.* **92** 5397
[62] Bader R F 1985 *Acc. Chem. Res.* **18** 9
[63] Henkelman G, Arnaldsson A and Jónsson H 2006 *Comput. Mater. Sci.* **36** 354
[64] Tang W, Sanville E and Henkelman G 2009 *J. Phys.: Condens. Matter* **21** 084204
[65] Maintz S, Deringer V L and Tchougréeff A L 2013 *J. Comput. Chem.* **34** 2557
[66] Deringer V L, Tchougréeff A L and Dronskowski R 2011 *J. Phys. Chem. A* **115** 5461
[67] Maintz S, Deringer V L and Tchougréeff A L 2016 *J. Comput. Chem.* **37** 1030
[68] Giannozzi P, Baroni S, Bonini N *et al.* 2009 *J. Phys.: Condens. Matter* **21** 395502
[69] Allen P B and Dynes R C 1975 *Phys. Rev. B* **12** 905

Supplementary Information:

Novel Superconducting Electrides in Ca–S System under High Pressures

Yun-Xian Liu(刘云仙), Chao Wang(王超),* Shuai Han(韩帅), Xin Chen(陈欣), Hai-Rui Sun(孙海瑞), and Xiao-Bing Liu(刘晓兵)*

†Laboratory of High Pressure Physics and Material Science (HPPMS), School of Physics and Physical Engineering, Qufu Normal University, Qufu, 273165, China

Computational Details

We have explored the pressure-induced structural evolution in Ca–S system with various Ca_mS_n (m = n = 1-4) using the CALYPSO and USPEX codes with simulation cell sizes of 1-4 formula units (f.u.) at temperature of 0 K and pressures at 0, 50, 100, 150 and 200 GPa. Such methods have been successfully employed in various systems. The CALYPSO structure searching: In the first step, random structures with certain symmetry are constructed in which atomic coordinates are generated by the crystallographic symmetry operations. After processing the first generation structures, 60% of them with lower Gibbs free energies are selected to construct the next generation structures by PSO (Particle Swarm Optimization). 40% of the structures in the new generation are randomly generated. A structure fingerprinting technique of bond characterization matrix is applied to the generated structures, so that identical structures are strictly forbidden. The energy convergence was set to 10-5 eV. The USPEX structure searching: In the evolutionary structural searching, the first generation of structures was always created randomly with its population size of 20-60 structures. The succeeding generations are produced by variation operator heredity (60%), lattice mutation (30%) and permutation (10%).

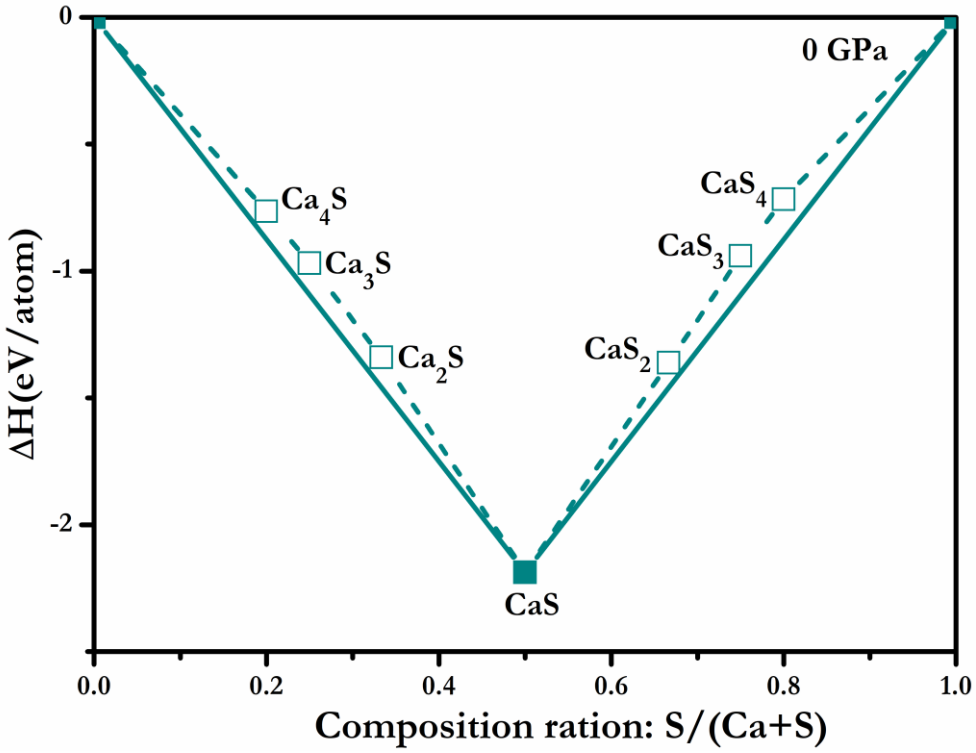

Figure S1. Calculated formation enthalpies of various Ca−S compounds at 0 GPa.

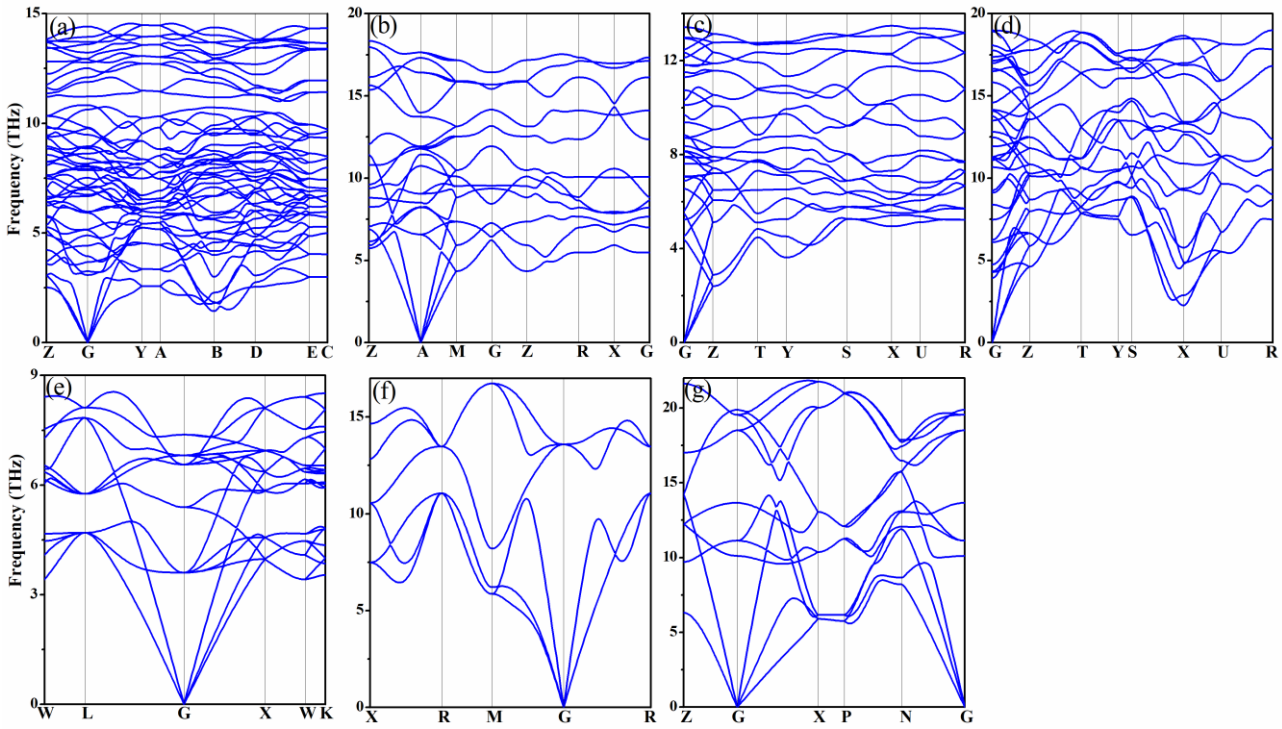

Figure S2. The calculated phonon spectra of the predicted stable Ca-rich compounds at selected pressures. (a) $P2_1/m$ Ca_3S at 60 GPa (b) $P4/mbm$ Ca_3S at 150 GPa (c) *Pnma* Ca_2S at 50 GPa (d) *Cmcm* Ca_2S at 150 GPa (e) *Fm*-3*m* CaS at 0 GPa (f) *Pm*-3*m* CaS at 100 GPa (g) $I4_1/amd$ CaS at 200 GPa.

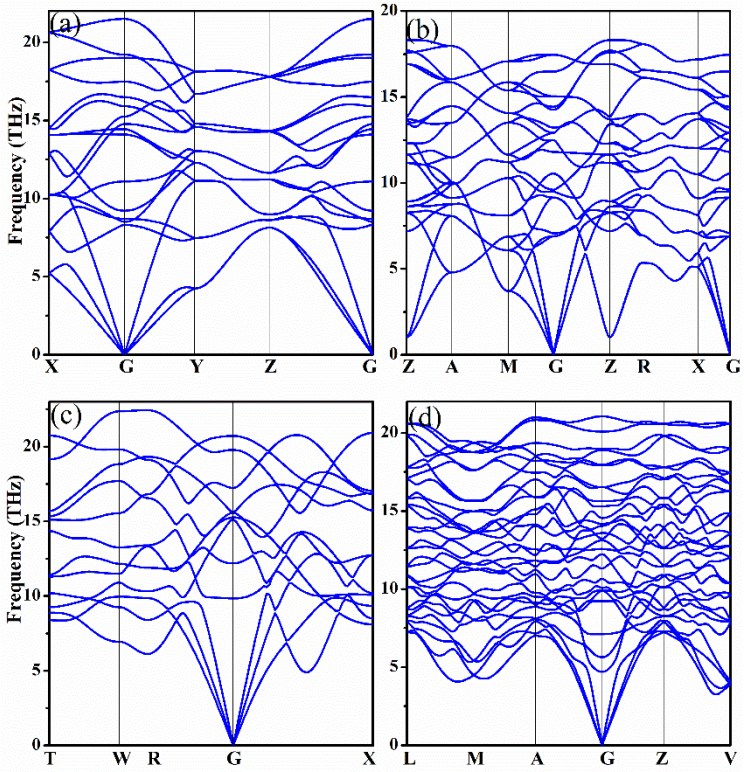

Figure S3. The calculated phonon spectra of the predicted stable S-rich compounds at selected pressures. (a) *Fddd* CaS_2 at 150 GPa (b) *P*-42_1m CaS_3 at 100 GPa (c) *Immm* CaS_3 at 200 GPa (d) *C*2/*c* CaS_4 at 200 GPa.

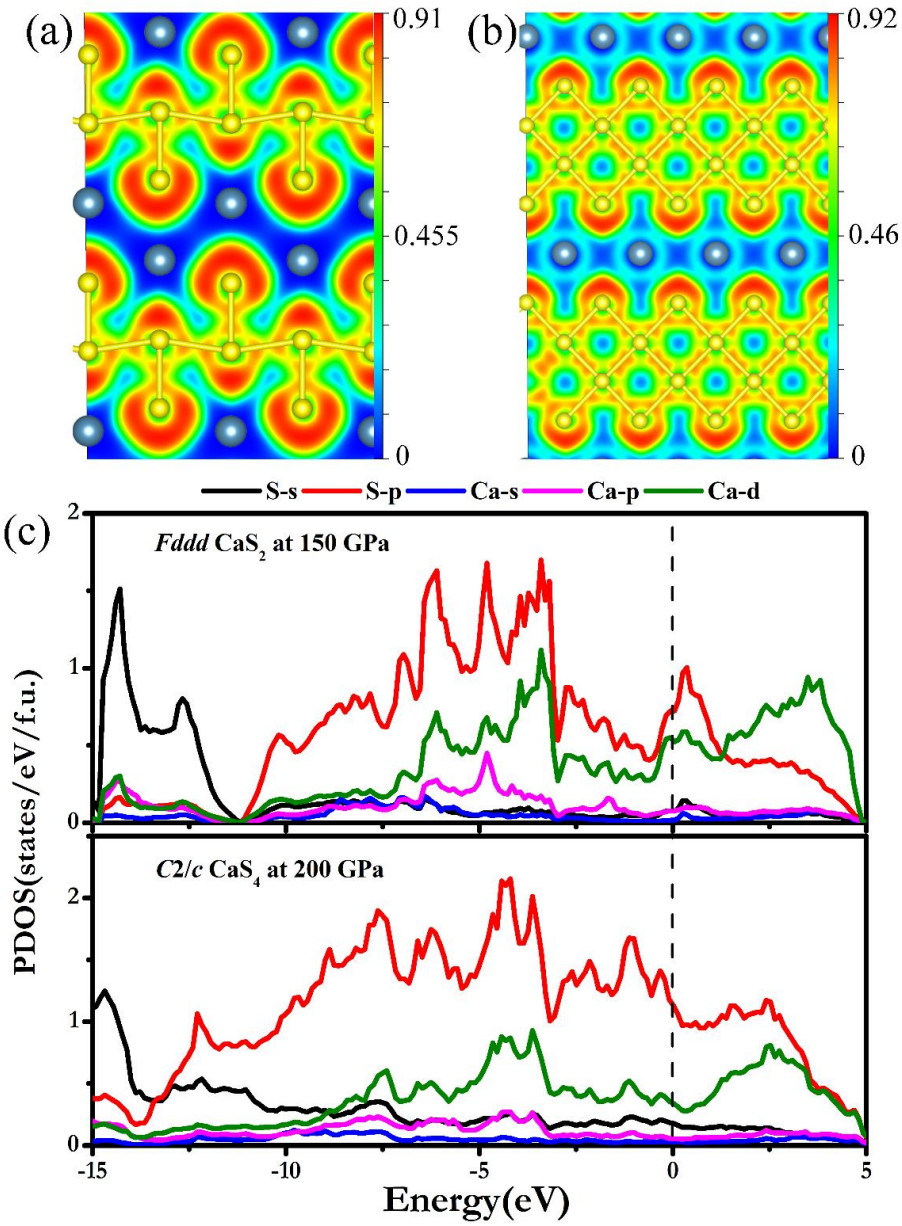

Figure S4. The calculated electron localization function (ELF) for CaS_2 and CaS_4. (a) *Fddd* CaS_2 (b) *C*2/*c* CaS_4 and (c) projected density of states (PDOS) for CaS_2 and CaS_4.

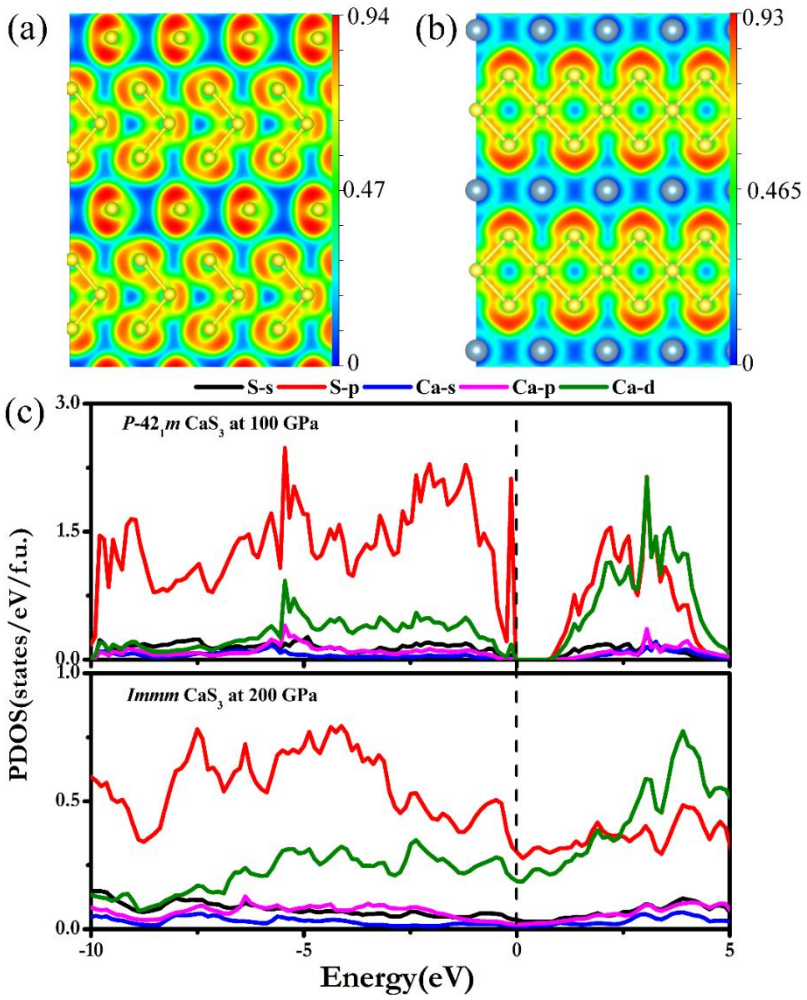

Figure S5. The calculated electron localization function (ELF) for CaS_3. (a) *P*-42_1m (b) *Immm* and (c) projected density of states (PDOS) for CaS_3.

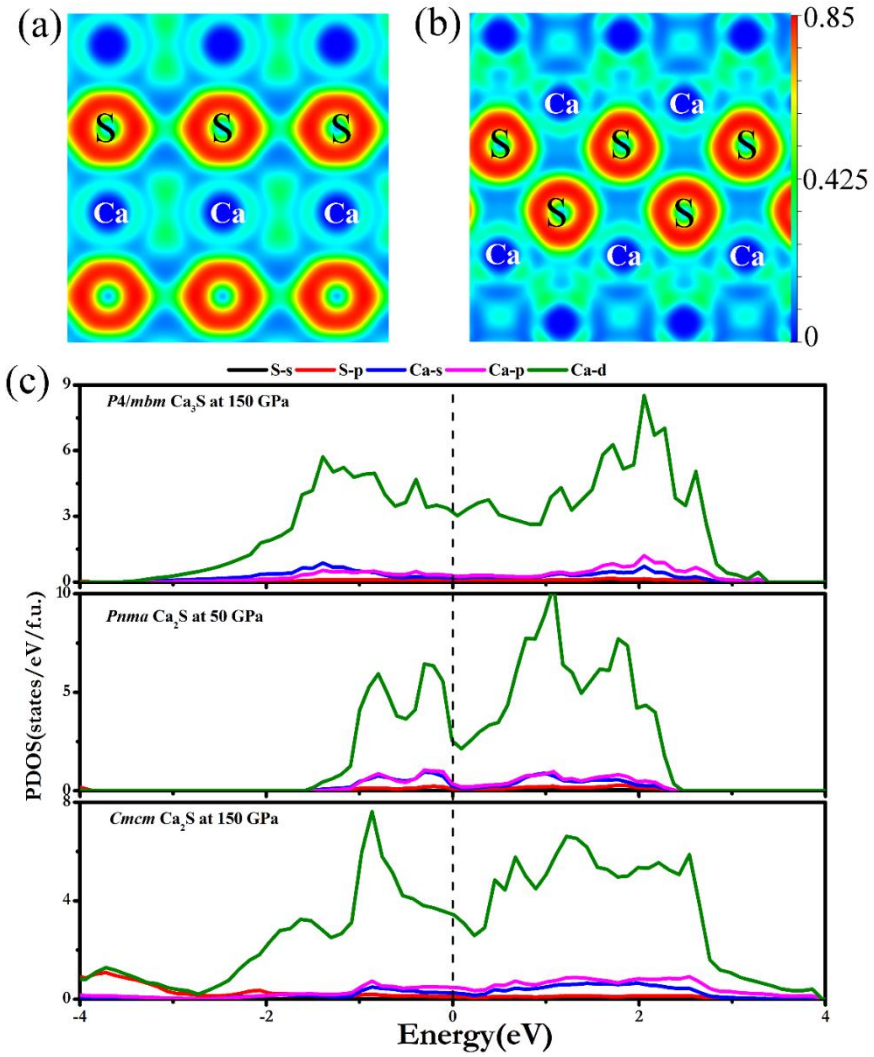

Figure S6. The calculated electron localization function (ELF). (a) *P*4/*mbm* Ca_3S (b) *Cmcm* Ca_2S and (c) projected density of states (PDOS) of *P*4/*mbm* Ca_3S, *Pnma* Ca_2S and *Cmcm* Ca_2S.

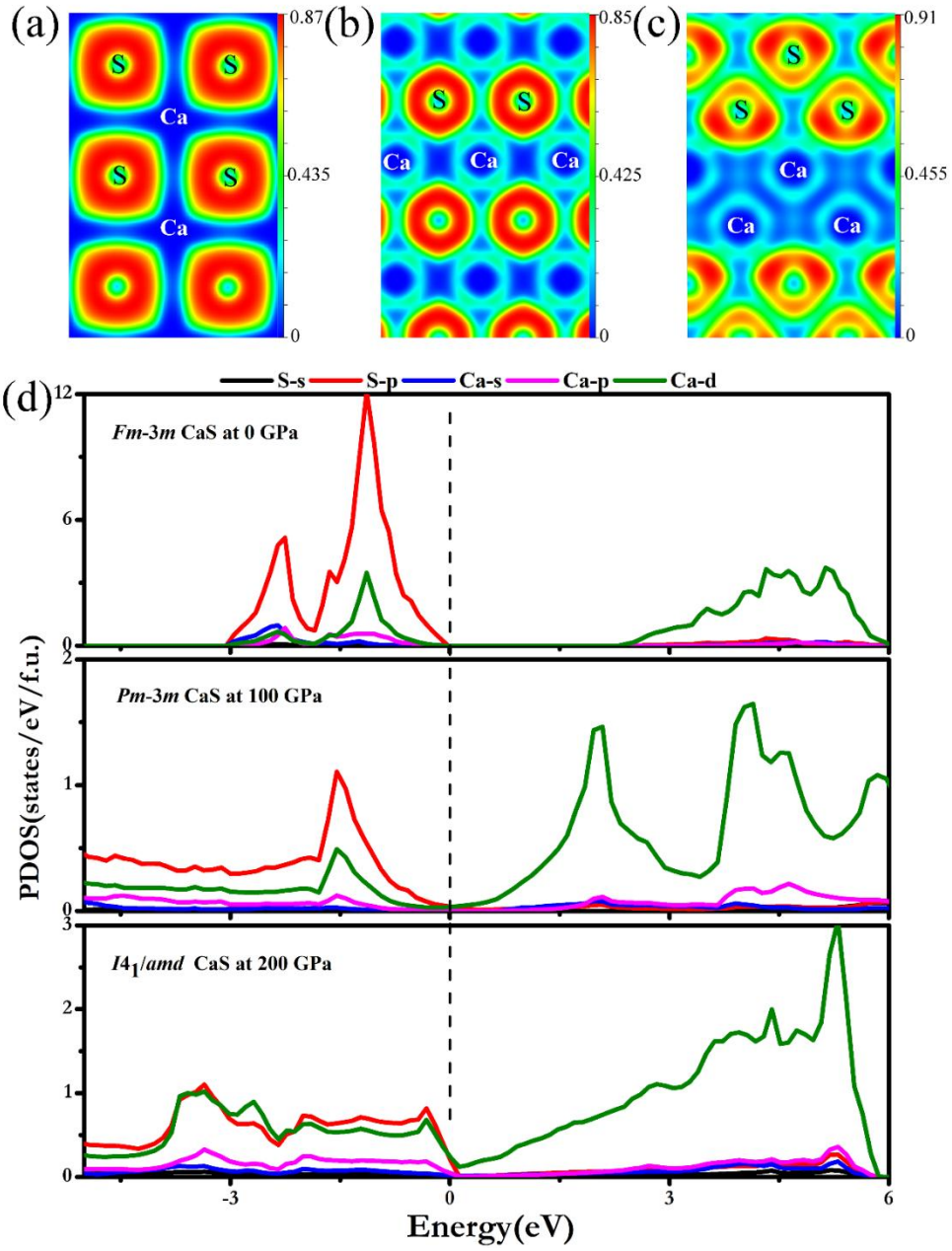

Figure S7. The calculated electron localization function (ELF) for CaS. (a) *Fm*-3*m* (b) *Pm*-3*m* (c) $I4_1/amd$ and (d) projected density of states (PDOS) for CaS.

Table S1 Structural parameters of Ca-S system at selected pressure.

Space group pressure	Lattice parameters (Å, °)	Atomic coordinates (fractional)	Sites
*P*2$_1$/*m* Ca_3S 50 GPa	a=11.7601 b=3.9581 c=5.2798 α=γ=90 β=95.413	Ca1 0.71746 0.75000 0.43627 Ca2 0.81856 0.25000 0.25522 Ca3 0.46173 0.75000 0.31037 Ca4 0.36082 0.25000 0.06974 Ca5 0.11197 0.25000 0.11684 Ca6 0.01756 0.75000 0.32048 S1 0.23980 0.75000 0.25497 S2 0.59000 0.25000 0.21484	2e 2e 2e 2e 2e 2e 2e 2e
*P*4/*mbm* Ca_3S 200 GPa	a=b=4.8148 c=3.2719 α=β=γ= 90	Ca1 0.30036 -0.80036 0.00000 Ca3 0.00000 -0.50000 -1.50000 S1 0.50000 -0.50000 -1.50000	4g 2c 2b
Pnma Ca_2S 100 GPa	a=4.9357 b=3.7499 c=7.8553 α=β=γ=90	Ca1 0.80971 0.25000 0.55808 Ca3 0.79889 0.25000 0.87482 S1 1.10750 0.75000 0.80442	4c 4c 4c
Cmcm Ca_2S 200 GPa	a=2.7546 b=10.6536 c=3.8931 α=β=γ= 90	Ca1 0.50000 0.22561 0.75000 Ca2 0.50000 0.42441 1.25000 S1 -0.00000 0.40158 0.75000	4c 4c 4c
Fm-3*m* CaS 0 GPa	a=b=c=5.7101 α=β=γ=90	Ca1 0.50000 0.50000 1.00000 S1 0.50000 0.50000 0.50000	4a 4b
Fm-3*m* CaS 100GPa	a=b=c=2.90180 α=β=γ=90	Ca1 -1.50000 -1.50000 -0.50000 S1 -1.00000 -1.00000 -1.00000	1b 1a
*I*4$_1$/*amd* CaS 200 GPa	a=b=3.3034 c=7.0815 α=β=γ= 90	Ca1 -1.00000 1.50000 0.25000 S1 -1.50000 0.50000 0.00000	4a 4b
Fddd CaS_2 200 GPa	a=7.4559 b=4.3278 c=6.8838 α=β=γ= 90	Ca1 0.75000 0.75000 0.25000 S1 0.25000 0.75000 0.10063	8a 16g
P-42$_1$*m* CaS_3 100 GPa	a=b=5.4158 c=3.0567 α=β=γ=90	Ca1 0.00000 -0.00000 -0.50000 S1 0.50000 -0.00000 -0.41780 S3 0.20088 0.70088 -0.99872	2b 2c 4e
Immm CaS_3 200 GPa	a=6.7265 b=3.8997 c=2.734 α=β=γ= 90	Ca1 -0.50000 -0.50000 -0.50000 S1 -0.21893 -0.50000 -0.00000 S9 -0.50000 -1.00000 -0.00000	2a 4f 2b
*C*2/*c* CaS_4 200 GPa	a=7.97428 b=2.86929 c=11.95417 α=γ=90 β=139.9	Ca1 0.00000 0.49966 0.75000 Ca2 0.50000 0.99966 0.75000 Ca3 0.00000 0.50034 0.25000 Ca4 0.50000 0.00034 0.25000 S1 0.88316 0.00020 0.33897 S2 0.66275 0.00030 0.01903 S3 0.38316 0.50020 0.33897	1a 1a 1a 1a 1a 1a 1a

		S4 0.16275 0.50030 0.01903 S5 0.11684 0.00020 0.16103 S6 0.33725 0.00030 0.48097 S7 0.61684 0.50020 0.16103 S8 0.83725 0.50030 0.48097 S9 0.11684 0.99980 0.66103 S10 0.33725 0.99970 0.98097 S11 0.61684 0.49980 0.66103 S12 0.83725 0.49970 0.98097 S13 0.88316 0.99980 0.83897 S14 0.66275 0.99970 0.51903 S15 0.38316 0.49980 0.83897 S16 0.16275 0.49970 0.51903	1a 1a 1a 1a 1a 1a 1a 1a 1a 1a 1a 1a 1a 1a 1a 1a